

## Synthetic Self-Assembling Clostridial Chimera for Modulation of Sensory Functions

Enrico Ferrari,<sup>†,‡</sup> Chunjing Gu,<sup>†</sup> Dhevahi Nirajan,<sup>†</sup> Laura Restani,<sup>§</sup> Christine Rasetti-Escargueil,<sup>||</sup> Ilona Obara,<sup>†,§</sup> Sandrine M. Geranton,<sup>†</sup> Jason Arsenault,<sup>†</sup> Tom A. Goetze,<sup>¶</sup> Callista B. Harper,<sup>□</sup> Tam H. Nguyen,<sup>□</sup> Elizabeth Maywood,<sup>†</sup> John O'Brien,<sup>†</sup> Giampietro Schiavo,<sup>●</sup> Daniel W. Wheeler,<sup>△</sup> Frederic A. Meunier,<sup>□</sup> Michael Hastings,<sup>†</sup> J. Michael Edwardson,<sup>¶</sup> Dorothea Sesardic,<sup>||</sup> Matteo Caleo,<sup>§</sup> Stephen P. Hunt,<sup>†</sup> and Bazbek Davletov\*,<sup>†,●</sup>

<sup>†</sup>MRC Laboratory of Molecular Biology, Cambridge, United Kingdom

<sup>‡</sup>School of Life Sciences, University of Lincoln, Lincoln, United Kingdom

<sup>§</sup>Istituto di Neuroscienze, Consiglio Nazionale delle Ricerche, Pisa, Italy

<sup>||</sup>National Institute for Biological Standard and Control, Health Protection Agency, Potters Bar, United Kingdom

<sup>†</sup>Department of Cell and Developmental Biology, University College London, London, United Kingdom

<sup>#</sup>School of Medicine, Pharmacy and Health, University of Durham, Stockton on Tees, United Kingdom

<sup>¶</sup>Department of Pharmacology, University of Cambridge, Cambridge, United Kingdom

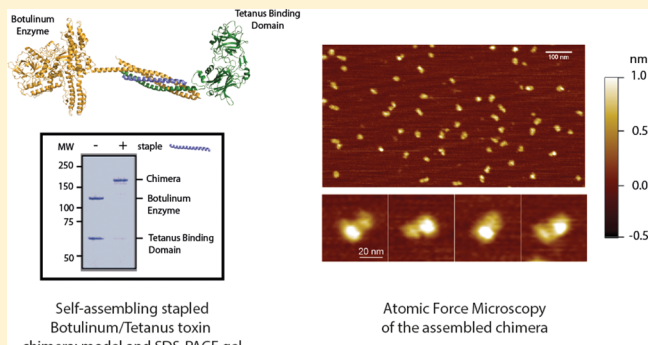
<sup>□</sup>The Queensland Brain Institute, University of Queensland, St Lucia, Australia

<sup>●</sup>London Research Institute, Cancer Research U.K., London, United Kingdom

<sup>△</sup>Department of Anaesthesia, Addenbrooke's Hospital, Cambridge, United Kingdom

<sup>●</sup>Department of Biomedical Sciences, University of Sheffield, Sheffield, United Kingdom

**ABSTRACT:** Clostridial neurotoxins reversibly block neuronal communication for weeks and months. While these proteolytic neurotoxins hold great promise for clinical applications and the investigation of brain function, their paralytic activity at neuromuscular junctions is a stumbling block. To redirect the clostridial activity to neuronal populations other than motor neurons, we used a new self-assembling method to combine the botulinum type A protease with the tetanus binding domain, which natively targets central neurons. The two parts were produced separately and then assembled in a site-specific way using a newly introduced ‘protein stapling’ technology. Atomic force microscopy imaging revealed dumbbell shaped particles which measure ~23 nm. The stapled chimera inhibited mechanical hypersensitivity in a rat model of inflammatory pain without causing either flaccid or spastic paralysis. Moreover, the synthetic clostridial molecule was able to block neuronal activity in a defined area of visual cortex. Overall, we provide the first evidence that the protein stapling technology allows assembly of distinct proteins yielding new biomedical properties.



### INTRODUCTION

Long-term and reversible silencing of selected central nervous system (CNS) areas and neuronal subpopulations in freely moving organisms would benefit both neuroscience and clinical medicine. One way to meet these difficult requirements is to re-engineer and utilize clostridial neurotoxins.<sup>1–3</sup> These toxins target neuronal synapses and neuromuscular junctions, enter presynaptic terminals, and then proteolyze unique SNARE proteins, thereby stopping neurotransmitter release.<sup>4–6</sup> Neuronal activity resumes when the proteolyzed proteins are replaced by *de novo* synthesized SNARE molecules in the active zones of presynaptic terminals.<sup>7,8</sup>

In nature, clostridial neurotoxins—produced by anaerobic *Clostridium* bacteria—selectively target motor functions to paralyze the intoxicated organism and gain a rich anaerobic environment upon the victim’s death. Seven botulinum toxins (designated A-G) from the genus *Clostridium botulinum* inactivate cholinergic motor neurons to cause flaccid paralysis.<sup>7</sup> The blood-brain barrier is impenetrable to botulinum neurotoxins and therefore all effects of botulinum poisoning are peripheral. In contrast to botulinum neurotoxins, tetanus toxin—

Received: July 11, 2013

Published: September 6, 2013

produced by *Clostridium tetani*—traverses motor neurons, via retrograde vesicular traffic,<sup>9</sup> to inactivate inhibitory interneurons in the spinal cord, causing rigid muscle paralysis.<sup>10</sup> This route to the spinal cord is utilized by *C. tetani* upon wound infection; but experimentally almost all central neurons (glutamatergic, glycinergic, etc.) can be targeted by tetanus toxin, leading to a blockade of neurotransmitter release.<sup>11</sup>

The major stumbling block in utilizing clostridial toxins for probing CNS functions is their life-threatening paralytic activity.<sup>10</sup> For example, when toxin is injected in a defined CNS area, its entry into the bloodstream can still lead to widespread paralysis. Clearly, non-motor-targeted versions of clostridial toxins would exclude paralytic actions and thus allow safe interrogation of CNS functions and new therapeutic applications. Our recent investigation of the reassembled botulinum neurotoxin type A, which carries an extended linker, demonstrated that it is as effective as native type A toxin in inactivating central neurons but has a reduced potency at neuromuscular junctions.<sup>12,13</sup> This was a fortuitous discovery, which could be accounted for by the reduced ability of the elongated toxin to enter tight neuromuscular junctions covered by Schwann cells. At high doses, the reassembled botulinum neurotoxin type A still causes flaccid paralysis (see Results section), and therefore we attempted to produce a truly nonparalytic neuronal blocker which combines the highly efficient botulinum protease and the CNS-targeting tetanus domain. Here we describe creation and properties of this new clostridial chimera which efficiently targets central neurons, blocks central nervous functions, and yet does not cause any paralysis.

## EXPERIMENTAL PROCEDURES

**Plasmids and Sequences.** mCherry fused to Tetanus toxin Binding Domain (TBD) was made by introducing the mCherry sequence from pmCherry-C1 vector (Clontech) into the EcoRI restriction site of pGEX-KG, followed by the *Clostridium tetani* TBD sequence (codon optimized for *E. coli* expression and synthesized by Eurogentec, from amino acids 856–1315 of the NCBI reference sequence NP\_783831.1) into the SacI restriction site. The plasmid for the expression of TBD fused to synaptobrevin was prepared by introducing the *Rattus norvegicus* synaptobrevin 2 sequence (codon optimized for *E. coli* expression and synthesized by Eurogentec, from amino acids 3–84 of the NCBI reference sequence NP\_036795.1) into the XhoI restriction site of pGEX-KG in front of the TBD sequence in the above pGEX vector. Botulinum neurotoxin A-derived LcTd-SNAP-25 has been described previously.<sup>12</sup> The *Rattus norvegicus* syntaxin 1 stapling peptide (amino acids 201–245 of the NCBI reference sequence NP\_446240.2) is C-terminally amidated and linked at the N-terminus to either fluorescein or TAMRA through an aminohexanoic acid spacer (synthesized by Peptide Synthetic, UK).

**Protein Preparation and Assembly Reaction.** mCherry TBD, botulinum LcTd-SNAP25, and synaptobrevin TBD were expressed in the BL21 strain of *E. coli*. Briefly, all proteins were expressed as GST C-terminal fusions cleavable by thrombin. Proteins fused to GST were purified on glutathione-Sepharose beads (GE Healthcare) and eluted from the beads in 20 mM Hepes, pH 7.3, 100 mM NaCl (Buffer A), using thrombin. Further purification was achieved by gel filtration using a Superdex 200 10/200 GL column (GE Healthcare). Protein concentration was determined using the BCA protein assay kit (Pierce). The clostridial chimera was assembled by mixing the

two clostridial fragments with the syntaxin peptide for 30 min at 20 °C, with each component at a 5 μM concentration, in the presence of 0.4% octyl glucoside. To visualize SNARE assemblies, SDS-PAGE was performed at 4 °C, and the gels were stained with Coomassie blue.

**Neuronal Cultures and Confocal Imaging.** Hippocampal neurons were cultured as previously described.<sup>14</sup> Briefly, the hippocampi were dissected from E18 BL21 mice and dissociated with 0.25% trypsin and trituration. The cells were counted and plated on 18-mm glass coverslips treated with 1 mg/mL poly lysine in borate buffer. The plating media was MEM (Gibco #11095) containing 0.6% glucose and 10% horse serum. After 3–4 h the coverslips were transferred to glia-conditioned media comprising Neurobasal (Gibco #21103) supplemented with glutamax and B27 serum-free supplement. The hippocampal neurons were used after 14 div and treated as previously described.<sup>15</sup> Neurons in Figure 3A were treated with fluorescein-linked chimera (10 nM) for 5 min in the presence of high K<sup>+</sup>, then fixed and processed for immunocytochemistry using an anti-synaptobrevin antibody. Coverslips were imaged using a Zeiss LSM 710 confocal microscope. Dorsal root ganglia (DRGs) neurons were prepared from neonatal Sprague–Dawley rats (2–8 days old) killed by cervical dislocation and then decapitated. Approximately 40–45 DRGs were removed from the vertebral column and transferred into Hank's Balanced Salt Solution (HBSS, Invitrogen). Nerve trunks and connective tissue were dissected away and the DRGs were placed in Neurobasal medium (Gibco, Life Technologies) containing 0.25% collagenase (type IV, Worthington) for 60 min at 37 °C. After washing with fresh Neurobasal medium (containing B27 supplement, Gibco, Life Technologies), ganglia were dissociated by trituration using a fire-polished Pasteur pipet. Cells were washed in fresh Neurobasal medium and triturated again using a smaller bore fire-polished pipet to produce a suspension of single cells. Cells were concentrated by centrifugation at 1000 r.p.m. (110 g) for 5 min and the resulting pellet was resuspended in neuronal culture medium containing B27 supplement, 1% penicillin–streptomycin solution, 1% L-glutamine, 100 ng/mL NGF (Alomone laboratories), and 2% cytosine β-D-arabinofuranoside (AraC, Sigma). The neuronal suspension was then slowly placed on poly(L-lysine) and laminin precoated glass bottomed culture dishes (MatTek Corporation) and incubated for 24 h at 37 °C in a humidified incubator gassed with 5% CO<sub>2</sub> in air. After 24–48 h of incubation, 10 nM TAMRA-linked chimera and 5 μg/mL Alexa Fluor 488-conjugated *Griffonia simplicifolia* IB4 (Invitrogen) were added to a 35 mm glass bottomed culture dishes. After a 15 min exposure in the dark, the culture was washed 3 times with clean Neurobasal culture medium before live imaging commenced. All live-cell images were taken with a confocal laser-scanning microscope (Zeiss LSM 710).

**AFM Imaging.** Purified clostridial chimera (500 nM) was diluted 50-fold in 100 mM NaCl, 50 mM Hepes-Na, pH 7.5; and 50 μL of the sample was allowed to adsorb to freshly cleaved mica disks for 10 min. The sample was washed with high purity water (Sigma-Aldrich) and dried under nitrogen. Imaging was performed with a Multimode atomic force microscope controlled by a Nanoscope IIIa controller (Bruker, Santa Barbara, CA, USA). Dry samples were imaged using the tapping mode. The silicon probes used (OMCL-AC160TS, Olympus, Tokyo, Japan) had a typical tip radius of 6.8 nm, a resonance frequency of ~300 kHz, and a spring constant of 40 N/m. The applied imaging force was kept as low as possible (between 85% and 90% of the free amplitude).

**Immunoblotting.** Hippocampal or DRG neurons were incubated for 20 h with the indicated concentration of either chimera or the control protein, lysed in 2% SDS, benzonase (250 U/mL, Novagen), 2 mM MgCl<sub>2</sub>, 60 mM Tris-HCl, pH 6.8. Botulinum-induced cleavage of SNAP-25 was evaluated by immunoblotting using an anti-SNAP-25 antibody (clone SMI 81, Covance) which recognizes both intact and cleaved SNAP-25. The percentage of the cleaved SNAP-25 was estimated by densitometry analysis using Quantity One software (Bio-Rad).

**Circadian Rhythms.** Organotypic slices of suprachiasmatic nucleus were obtained from neonatal mice (10 days of age) carrying a knock-in mutation of the Period2 circadian clock gene that encodes Per2-luciferase fusion protein.<sup>16</sup> Following a 3-day initial period to confirm robust circadian oscillation, the slices were bath treated with 5 nM of the clostridial chimera and recording continued for further 9 days. Per2-driven bioluminescence was recorded using photomultiplier tubes (Hamamatsu), as described elsewhere.<sup>17</sup>

**Hemidiaphragm Assay.** Left phrenic nerve-hemidiaphragm preparations from male inbred mice (Balb/c) were incubated in a 37 °C bath containing the Krebs-gelatin buffer gassed with 95% O<sub>2</sub>/5% CO<sub>2</sub>. Muscle contractions triggered by stimulation of the nerve with a supra-maximal voltage (~3 V, 1 Hz, 0.2 ms) were measured using an isometric force transducer (FMI, Seeheim, Germany) linked to a bridge amplifier ML110 and a Powerlab/4SP 4 channel recorder (ADIstruments, Chalgrove, UK). The hemidiaphragm resting tension was increased stepwise during the equilibration period until a reproducible twitch was observed. Once the muscle twitch responses to nerve stimulation had stabilized and were of constant size for at least 30 min, the Krebs solution was replaced with one containing native type A toxin or reassembled toxin and stimulation resumed. The decrease in contraction was calculated in relation to the contractions just before toxin addition.<sup>18</sup> Native botulinum neurotoxin (580 pM) used for reference (HPA, Potters Bar, UK) had efficacy of 20 000 LD<sub>50</sub>/mL.

**Biological Testing.** Adult C57 BL6 mice (20–25 days of age; average weight 20 g) were injected intravenously or intramuscularly with the clostridial chimera or reassembled botulinum neurotoxin (500 ng). The proteins were diluted in Hartmann's Solution to achieve a required dose for the injection volume of 50 μL. Animals were replaced in their cages and monitored every 6 h for 4 days. The end point of the experiment was the appearance of weakness of the musculature of the limbs either ipsilateral to the injection point or bilaterally. Surviving animals were sacrificed after 7 days.

**Visual Cortex Experiments.** A portion of the skull overlying the occipital cortex was drilled on one side of the skull. The injections into the visual cortex were done using a glass micropipet, connected to an injector, at the following coordinates (in mm with respect to lambda): AP, 0; ML, 4.5; 1.2 below dura.<sup>19</sup> Clostridial chimera (50 nM, 1 μL, equivalent to 7.5 ng) or vehicle (rat serum albumin 2%, in PBS, 1 μL) was injected into the visual cortex of P40 Long Evans rats. Electrophysiological, anatomical, and biochemical analyses were performed 4–8 days after toxin delivery. For electrophysiological recordings, rats were anesthetized with Hypnorm/Hynovet (3.75 mL/kg body weight) and placed in a stereotaxic apparatus. Recordings were performed as described previously.<sup>19,20</sup> Both eyes were fixed by means of adjustable metal rings surrounding the external portion of the eye bulb, and optic disk locations were projected onto a tangent screen to determine the vertical meridian. Body temperature during the experiments

was constantly monitored with a rectal probe and maintained at 37 °C with a heating blanket. The electrocardiogram was also continuously monitored. A portion of the skull overlying the occipital cortex was drilled on one side of the skull, and a tungsten electrode (FHC; 1 MΩ) was mounted on a three-axis motorized micromanipulator and inserted into the portion of the visual cortex previously injected with clostridial chimera (4.5 mm lateral from midline and in correspondence with lambda). Visual evoked potentials (VEPs) were recorded at depths of 100 and 400 μm within the cortex. Steady-state VEPs were recorded in response to reversal (4 Hz) of a horizontal sinusoidal grating (spatial frequency, 0.07 cycles/deg; contrast 10%, 20%, 30%, 90%), generated by computer on a display (Sony; 40 × 30 cm; mean luminance 15 cd/m<sup>2</sup>) by a VSG card (Cambridge Research Systems). Signals were amplified (1000-fold), band-pass filtered (0.5–100 Hz), and fed into a computer for storage and analysis. At least 80 events were averaged in synchrony with the stimulus contrast reversal. VEP amplitude was quantified by measuring the amplitude of the second harmonic of the Fourier transform computed from the recorded signal, as previously described,<sup>21</sup> using a custom-made application based on the LabView software. The response to a blank stimulus (0% contrast) was also frequently recorded to estimate noise. In each animal, contrast threshold curves were measured close to (<500 μm) or far from (>500 μm) the injection site. In each animal, at least six penetrations were performed (3 'close to' and 3 'far from' the injection). Visual responsiveness was determined as the signal-to-noise ratio, that is, the ratio between VEP amplitude at a given contrast and blank amplitude. In each animal, we compared visual responses close to and far from the injection by plotting a contrast threshold curve, in which responsiveness at a given contrast was normalized to the values measured at 90% contrast in penetrations distant from the delivery site. Analysis of VEP responses was performed blind to experimental treatment. For immunohistochemistry, the animals were deeply anesthetized with chloral hydrate and perfused through the heart with freshly prepared 4% paraformaldehyde in 0.1 M phosphate buffer, pH 7.4. Tissues were dissected and postfixed for 2 h at 4 °C. Brain sections (40 μm thick) were cut with a microtome. Sections were blocked with 10% normal horse serum in PBS containing 0.25% Triton X-100 and then incubated overnight at room temperature with a rabbit polyclonal antibody to cleaved SNAP-25 (1:200 dilution; kind gift of O. Rossetto, University of Padua, Italy). On the following day, sections were incubated with Rhodamine Red X-conjugated secondary antibody (1:500, Jackson ImmunoResearch) for 2 h at room temperature. Sections were washed in PBS and incubated for 5 min with YoYo-1 (1:500 in PBS; Invitrogen), then washed again in PBS and mounted using an antifading agent (Vectashield; Vector Laboratories). Images were acquired using a Leica confocal laser-scanning microscope and a 10× objective. Immunoblotting was performed as described previously.<sup>22,23</sup> Cortical parts were excised and lysed using a buffer containing 1% Triton X-100, 10% glycerol, 150 mM NaCl, 10 mM EDTA, 0.1 mM Na<sub>3</sub>VO<sub>4</sub>, 1 μg/mL leupeptin, 1 μg/mL aprotinin, 1 mM PMSF, and 20 mM Tris-HCl, pH 7.5. Proteins (10 μg) were separated by electrophoresis and transferred to blotting paper, which was then incubated with primary antibody overnight at 4 °C (anticleaved SNAP-25, 1:500 dilution; antitubulin antibody 1:15 000 dilution, Sigma). Blots were then reacted with HRP-conjugated secondary antibodies (Jackson ImmunoResearch) and developed using an enhanced chemiluminescence kit (GE Healthcare).

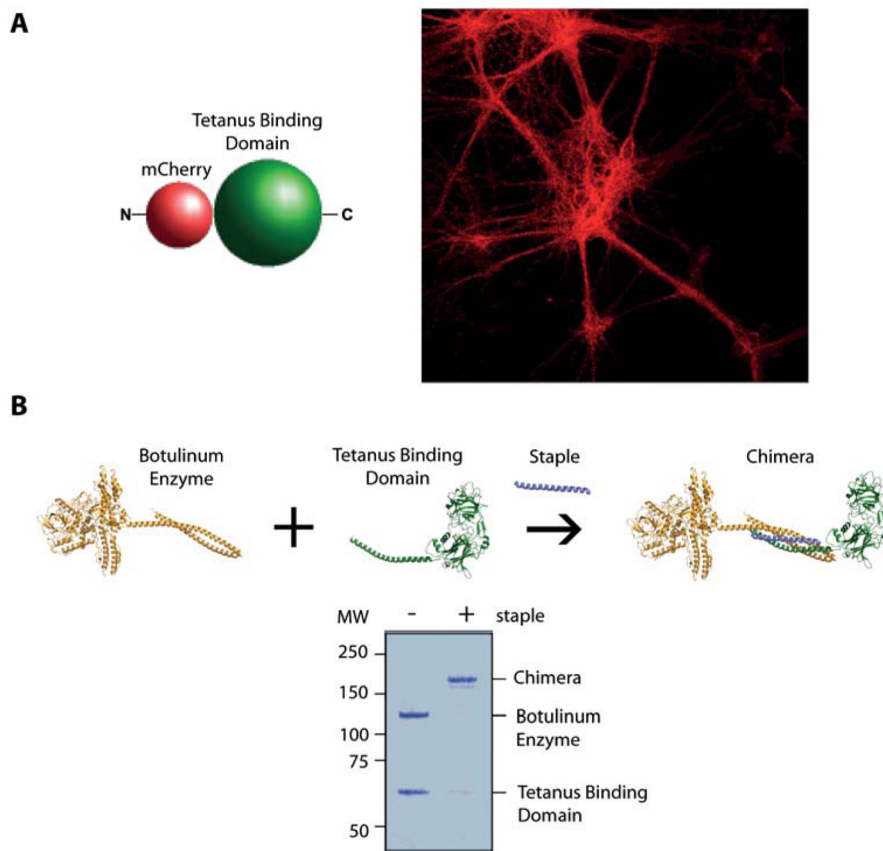


**Figure 1.** Assembly of the tetanus-botulinum chimera from two components. (A) mCherry-tagged tetanus binding domain (left) efficiently binds mouse hippocampal neurons in culture within 20 min (right). (B) Botulinum enzyme type A was stapled to the tetanus receptor binding domain using a fluorescently labeled stapling peptide (top schematic). Coomassie-stained SDS-PAGE gel (bottom) showing assembly of the clostridial chimera in the presence of the stapling peptide in a 30-min reaction. The stapled product is resistant to SDS indicating an irreversible assembly.

**Inflammatory Pain Experiments.** Experiments were carried out on male Sprague–Dawley rats ( $\sim 200$  g body weight at the beginning of the experiment) from the colony at University College London. Animals were housed in their home cage controlled for temperature ( $21$  °C) and humidity (55%) under a regular 12-h day/night cycle (lights on at 8:00 a.m.; lights off at 8:00 p.m.). Standard laboratory rodent chow and water were available *ad libitum*. Animals were habituated to testing procedures for at least 3–4 days before experiments. For intrathecal (i.th.) injections, rats were anesthetized using 2% isoflurane with oxygen as the carrier gas (1 L/min). Rats were placed in a stereotaxic frame and a small incision was made in the atlanto-occipital membrane. A cannula was inserted into the subarachnoid space, terminating in the L4–L5 region. Animals received either 10  $\mu$ L of clostridial chimera (100 ng) or vehicle (saline). The cannula was then withdrawn and the wound closed with suture clips. Local inflammation was induced by intraplantar (i.pl.) injection of CFA (Sigma, Poole, UK; 50  $\mu$ L) into the left plantar surface of the hind paw, under isoflurane anesthesia as above. During the injection the needle penetrated the skin just distal to the targeted area and terminated at the center of the plantar surface of the left hind paw. To assess mechanical sensitivity following the development of inflammation, withdrawal responses were measured with an automatic Von Frey apparatus (Ugo-Basile, Italy). Animals were left to habituate to the experimental room in their home cage for 20 min before the beginning of each testing session. Each animal was tested 4 times with a resting time of 5–10 min between each measurement. For

the automatic Von Frey, the ramp was set to reach the maximum stimulus of 50 g in 20 s. Mechanical threshold at the central plantar surface of the hind paw was assessed before the chimera and CFA injections (as a basal pain threshold). The chimera was first injected intrathecally and the mechanical threshold was assessed 3 days after the injection. Then, in the same group of rats CFA was injected i.pl. and behavioral testing continued between 2 h and 11 days after CFA. During testing the observer was blinded to the i.th. treatment. Data analysis and statistical comparisons were performed using GraphPad Prism (GraphPad Software, USA). Results are presented in the graphs as % of control (basal pain threshold prior the i.th. injection)  $\pm$  SEM. Statistical analysis was performed by two-way analyses of variance (ANOVA) with Bonferroni's multiple comparison posthoc tests,  $n = 6$ . A value of  $p < 0.05$  was considered to be statistically significant.

**Ethics Statement.** Animal experiments were carried out under license from the UK Home Office in accordance with the Animals (Scientific Procedures) Act 1986 and in accordance with the European Community Council Directive of November 24, 1986 (86/609/EEC).

## RESULTS

To assess the ability of our fully synthetic tetanus toxin binding domain (TBD) to bind central neurons, we prepared mCherry-fused TBD as a single recombinant protein and incubated it with cultured rat embryonic hippocampal neurons for 30 min. Figure

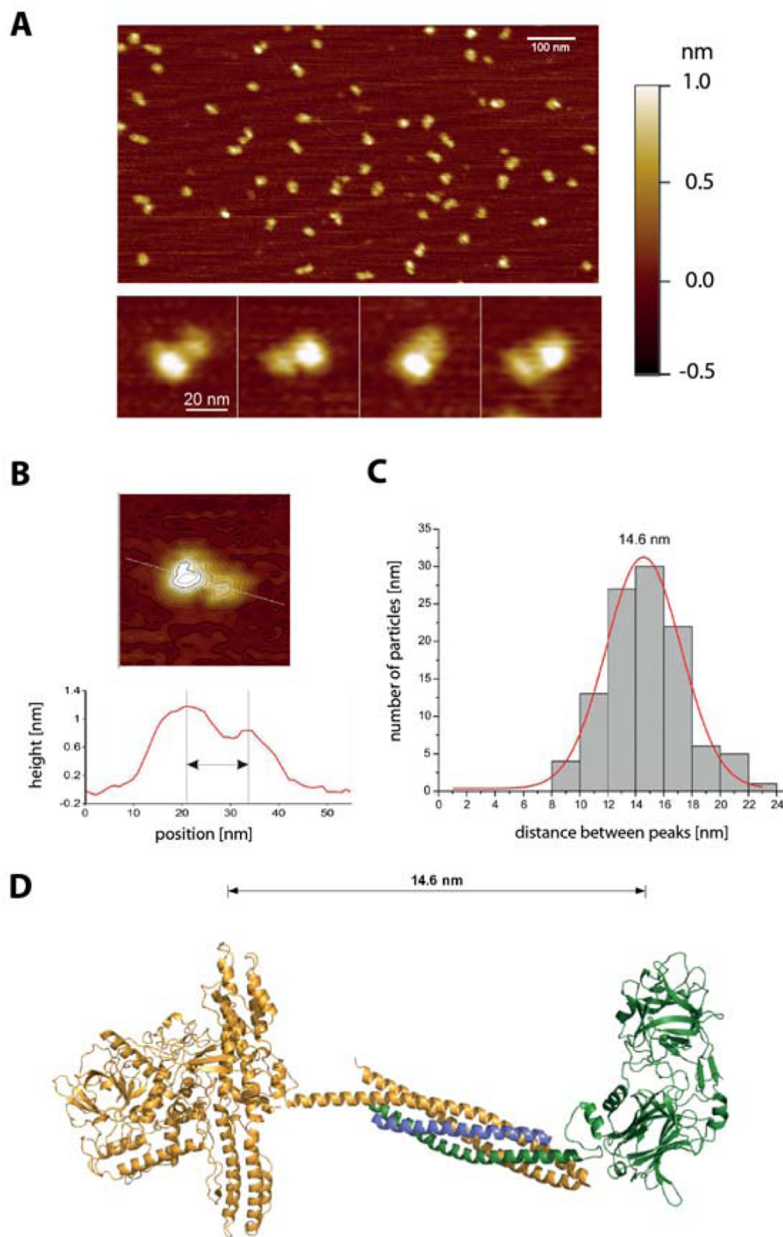


**Figure 2.** AFM imaging of the clostridial chimera. (A) AFM image showing a field view of the stapled clostridial chimera (upper panel, scale bar 100 nm). Four representative enlarged images of the clostridial chimera demonstrating the dumbbell-like shape of the molecule (lower panel, scale bar 20 nm). The color-coded bar (right) indicates the height of the probed surface. (B) Single-molecule analysis of particles from selected topography images (upper panel). The height profile along the major axis (white line) was plotted and the peak-to-peak distance measured. (C) The distribution of a large number of particles' peak-to-peak distances ( $N = 108$ ) has been plotted and fitted to a Gaussian curve, which has a mean value of 14.6 nm. (D) Molecular model of the clostridial chimera generated using the following structures available in the Protein Data Bank archive (<http://www.rcsb.org>): 3BTA (BoNT/A), 1N7S (SNARE complex), 1FV2 (TBD). The protein sequences have been truncated and/or joined according to the 'Plasmids and sequences' section in the Experimental Procedures and then oriented and assembled using PyMol. The average peak-to-peak distance of 14.6 nm, obtained from the single-molecule analysis, is visually compatible with the structure of the molecular model.

1A shows that mCherry-TBD bound to hippocampal neurons in a robust way.

Next, we assembled the clostridial chimera from two separately prepared parts: (i) botulinum type A protease/translocation unit fused to a linker polypeptide, and (ii) TBD fused to a complementary linker. The two linkers utilize SNARE-derived peptides, which assemble spontaneously within minutes in the presence of a stapling peptide.<sup>24,25</sup> Figure 1B shows the typical assembly reaction as visualized by SDS-PAGE. As expected from

the uniquely irreversible reaction, the chimera made of two independent clostridial parts exhibited SDS-resistant properties.

Next we assessed the assembled clostridial chimera using atomic force microscopy (AFM), which demonstrated uniform dumbbell-shaped particles (Figure 2A). The topographic image of individual particles and the profile of the measured height along their major axis presented two peaks, likely corresponding to the two assembled clostridial chimera parts (Figure 2B). Single-molecule analysis of a large number of individual particles resulted in an average peak-to-peak distance of 14.6 nm (Figure

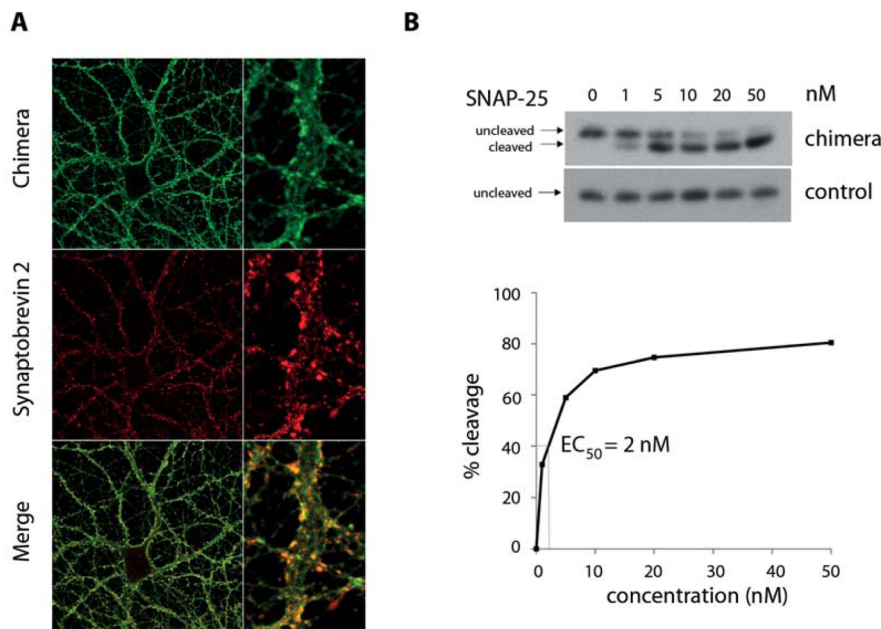


**Figure 3.** The clostridial chimera penetrates synaptic endings and cleaves intraneuronal SNAP-25. (A) Confocal microscopy images ( $63\times$  magnification) showing colocalization of the fluorescein-labeled chimera (green) with a synaptic vesicle marker, synaptobrevin (red), following KCl-induced stimulation of cultured hippocampal neurons. Right panels show digitally zoomed details from the confocal images on the left. (B) Immunoblot showing cleavage of SNAP-25 by the botulinum enzyme in hippocampal neurons following addition of the clostridial chimera at the indicated concentrations (upper panel). Control reactions were carried out using the botulinum enzyme without tetanus binding domain. The graph (lower panel) shows quantification of the SNAP-25 cleavage measured by densitometry of the above immunoblot and indicates the EC<sub>50</sub> for the chimera-induced proteolysis being 2 nM.

2C). This value is consistent with the molecular model depicted in Figure 2D. In this model the length of 14.6 nm equals the distance between the approximate geometrical centers of the botulinum protease/translocation unit and the TBD, assuming they are kept apart and oriented by the assembled SNARE complex. The molecular model, supported by the single-molecule analysis, allowed us to estimate an apparent length of the clostridial chimera of  $\sim$ 23 nm.

To test the ability of the chimera to enter the nerve endings of central neurons,<sup>26,27</sup> we added it to cultured hippocampal neurons and activated the neurons using 50 mM potassium chloride for 10 min. The presynaptic uptake of the clostridial chimera was assessed by colocalization with a synaptic vesicle marker, synaptobrevin. Confocal microscopy of the neurons revealed robust internalization of the chimera into the synaptic endings of neurons (Figure 3A). Clostridial neurotoxins block synaptic transmission by cleaving SNARE proteins at defined sites: the botulinum type A enzyme removes only 9 amino acids from the C-terminus of the intraneuronal SNAP-25 protein, and yet this is sufficient to block neurotransmitter release.<sup>10</sup> The ability of the clostridial chimera to translocate its botulinum enzyme and cleave SNAP-25 was evaluated by immunoblotting. Figure 3B shows that neuronal SNAP-25 was efficiently cleaved by the chimera at concentrations in the low nanomolar range, confirming functionality of the assembled molecule.

To evaluate the biological activity of the chimera, we applied it to mouse suprachiasmatic nucleus organotypic brain slices, which exhibit circuit-driven circadian rhythms visualized using a luciferase activity.<sup>17</sup> Figure 4A shows that application of the chimera at 5 nM led to a strong inhibition of circadian rhythms, confirming its ability to affect native neuronal circuits. We previously noted that structurally extended botulinum toxin type A has a significantly reduced paralytic ability, most likely because

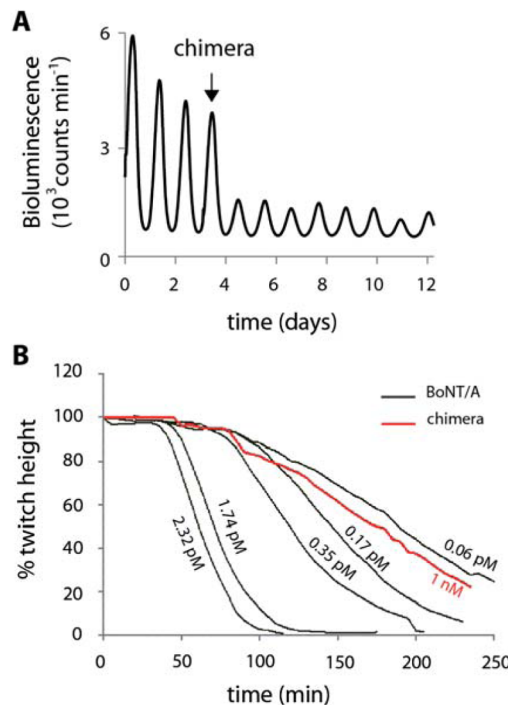


**Figure 4.** Functional testing of the clostridial chimera in mouse tissues ex vivo. (A) Circadian rhythms in *ex vivo* cultured mouse suprachiasmatic nucleus, visualized using a luciferase activity, are significantly damped following application of the clostridial chimera (5 nM). (B) Comparison of the paralytic ability of the clostridial chimera and native botulinum toxin type A (BoNT/A). Muscle twitch responses to nerve stimulation were recorded for up to 4 h following application of BoNT/A and the clostridial chimera at the indicated concentrations.

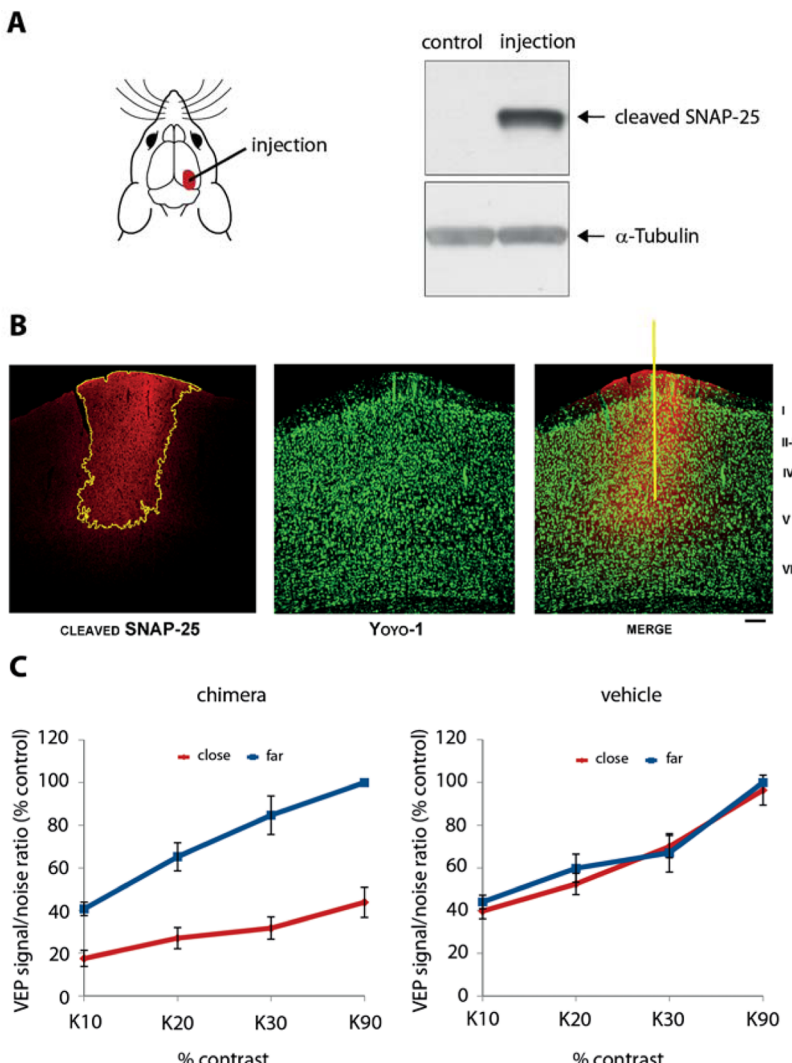


**Figure 5.** Clostridial chimera attenuates brain activity following localized injection into the rat visual cortex. (A) Schematic diagram showing the injection site of the chimera (left). The brain areas tested were subjected to immunoblot analysis revealing the cleaved SNAP-25 product only in the chimera-injected, but not in vehicle-treated cortex (control). Staining with the anti- $\alpha$ -tubulin antibody indicates equal loading of brain-derived material. (B) Confocal microscopy images of immunostained brain slices showing localized cleavage of SNAP-25 (in red) 4 days following the injection. The yellow contour delineates an intense immunofluorescence observed for the cleaved SNAP-25 product (left panel). YoYo-1 nuclear staining (green) was used to highlight the brain structure (middle panel); the yellow line in the right panel indicates the pipet track. Scale bar = 120  $\mu$ m. (C) The amplitude of visual evoked potentials (VEPs) as a function of variable contrast (K20–K90) is strongly reduced following the injection of the chimera (left,  $n = 5$ ) but not the vehicle (right,  $n = 4$ ) in the visual cortex. The internal standard in each experiment consisted of VEPs measured far ( $>500$   $\mu$ m) from the injection site (blue). In vehicle-injected rats there is no difference between contrast curves measured either close to (red) or far from (blue) the injection site (two-way ANOVA,  $p = 0.41$ ). On the contrary, in the chimera-injected rats, the contrast curve recorded at the injection site displays significantly lower VEP values (two-way ANOVA,  $p = 0.006$  followed by Holm-Sidak test,  $p < 0.05$ ). Data are expressed as mean  $\pm$  SEM.

of its inability to reach/penetrate neuromuscular junctions.<sup>13</sup> Indeed while the LD<sub>50</sub> of the native BoNT/A in mice is  $\sim$ 5 pg, peritoneal injections of  $\sim$ 5 ng had no lethal effect in mice.<sup>13</sup> Further experiments, however, revealed that when injected in mice in the range of 100–500 ng, the stapled botulinum toxin leads to typical signs of botulism and death (data not shown).

We used isolated mouse hemidiaphragm muscles to assess the paralysing ability of the new clostridial chimera. Figure 4B shows that while picomolar amounts of native botulinum toxin readily blocked muscle twitching, the clostridial chimera could only achieve this effect at nanomolar concentrations. We estimated from the fitted LD<sub>50</sub> curve that the clostridial chimera is 11 000 times less effective than the native toxin in causing neuromuscular paralysis. To confirm the nonparalytic nature of the chimera, we injected it either in a mouse thigh or intravenously at

500 ng, that is, 100 000-fold higher than the LD<sub>50</sub> of native botulinum toxin. All mice ( $n = 6$ ) survived the injections and none exhibited signs of paralysis.

Long-acting nonparalytic neuronal blocking agents could be an excellent tool for silencing selected brain areas or spinal regions both in research and in medicine, for example, for treatment of drug-resistant epilepsy or chronic pain. For this reason, we evaluated the ability of the chimera to inhibit cortical activity in the rat visual cortex. The chimera (1  $\mu$ L containing 7.5 ng) was pressure-injected in layer V of the visual cortex and clostridial activity was first assessed by tissue immunoblotting and brain slice immunostaining, using an antibody that recognizes only the cleaved SNAP-25 product.<sup>28</sup> Figure 5A shows that the cleaved SNAP-25 can only be detected in the injection site, being restricted to a small area of the visual cortex

extending from layer V up to the pipet penetration point. Lateral spread of toxin (delineated in yellow in Figure 5B) was consistently less than 1 mm in coronal sections of the infused hemisphere. Next, visually evoked potentials (VEPs) were recorded either around the toxin delivery site or at a distance >500  $\mu$ m from the injection, 4–8 days after toxin delivery. We found that visual responsiveness (i.e., the VEP signal-to-noise ratio<sup>21,29</sup>) was substantially dampened within the affected cortex as compared to distant regions (Figure 5C, left). VEPs were significantly reduced across a range of stimulus contrasts (two-way ANOVA,  $p = 0.006$ , followed by Holm Sidak test,  $p < 0.05$ ; Figure 5C, left). No alterations in visual responsiveness in the treated area were found in animals injected with vehicle solution (two-way ANOVA,  $p = 0.41$ ; Figure 5C, right), confirming that the new clostridial chimera can attenuate neuronal activity in a small, selected area of the brain.

The most promising use of long-acting nonparalytic neuronal blocking agents would be in the treatment of prolonged pain.<sup>30</sup> We evaluated the ability of the clostridial chimera to reduce mechanical hypersensitivity triggered by injection of an inflammatory substance into the hind paw of rats. The clostridial chimera (100 ng) was delivered at the L4-L5 level of the rat spinal cord intrathecally in a volume of 10  $\mu$ L. Following the injections, rats exhibited neither spastic nor flaccid paralysis, indicating that tetanic muscle spasms are a specific feature of the motor neuron route that tetanus toxin normally exploits to reach the ventral horn of the spinal cord.<sup>10</sup> Three days after the clostridial chimera injections, basal mechanical sensitivity thresholds were evaluated using an automatic von Frey apparatus. This revealed no change in acute mechanical nociception (Figure 6A).

Next, these rats were injected with Complete Freund's Adjuvant (CFA) into the hind paw and inflammation-induced mechanical hypersensitivity was assessed for up to 11 days (Figure 6A). Compared to the control group injected with saline, rats that had received intrathecal injection of the chimera exhibited significant reduction of mechanical hypersensitivity. This effect was observed from 24 h after CFA injection and lasted for as long as 11 days after CFA injection, which can be explained by the long-lasting botulinum proteolytic effects.<sup>2,10</sup> To determine the proportion of sensory neurons affected, we exposed cultured rat dorsal root ganglion neurons to the chimera and assessed cleavage of SNAP-25 using an antibody against the intact N-terminus of SNAP-25.<sup>31</sup> Figure 6B shows that even at high concentrations approximately half of the SNAP-25 remained intact, suggesting that a population of sensory neurons is resistant to the chimera. It has been reported that mechanical sensitivity is transduced by the IB4-lectin-binding neurons.<sup>32</sup> We evaluated whether the IB4 lectin and the TBD bind the same population of dorsal root ganglion neurons. Remarkably, the TBD and IB4 bound to two populations of sensory neurons in a mutually exclusively manner (Figure 6C). This result indicates that pain-conducting mechanoreceptors in the rat belong to tetanus- rather than IB4-binding neurons.

## ■ DISCUSSION

Silencing selected neuronal populations in defined areas of the CNS is important for both research and medicine. Clostridial molecules which inactivate the synaptic release machinery offer an opportunity to design long-acting neuronal blocking agents. The first step toward utilization of clostridial molecules for selective neuronal blockade is to remove their highly potent neuromuscular paralytic activity. Here we present the first clostridial chimera which does not cause muscle paralysis in

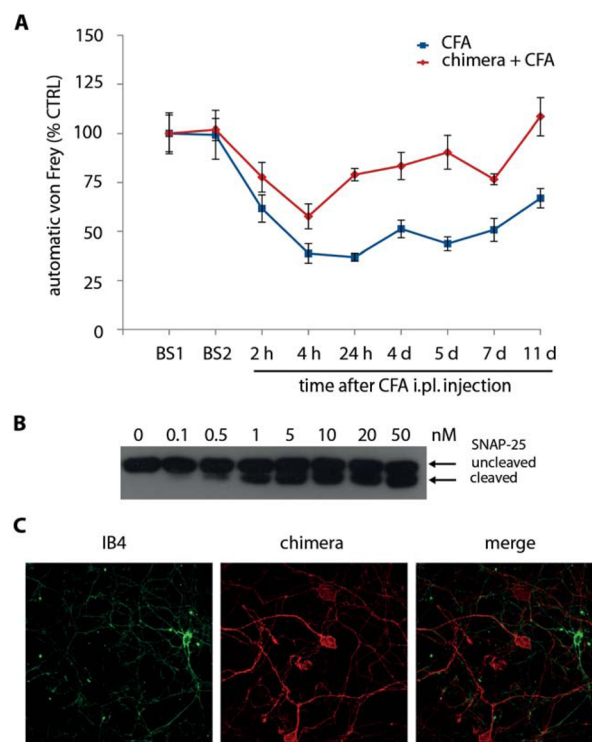


**Figure 6.** Intrathecally delivered clostridial chimera reduces mechanical hypersensitivity in a rat model of inflammatory pain. (A) Graph showing relative rat paw mechanical sensitivity measured using an automatic von Frey apparatus. The clostridial chimera (100 ng) was injected intrathecally (i.th.) at the L4-L5 level of spinal cord (red diamonds,  $n = 6$ ). Control rats (blue squares) received i.th. injection of vehicle (saline). CFA was injected into left hind paw (intraplantar, i.pl.) and mechanical hypersensitivity was assessed between 2 h and 11 days after CFA. BS1 – basal pain threshold prior to i.th. injections; BS2 – basal pain threshold three days after i.th. injections. Data are expressed as % of control (basal pain threshold prior to the i.th. injection)  $\pm$  SEM. (B) Immunoblot showing that the clostridial chimera even at high concentrations cleaves only 50% of neuronal SNAP-25, suggesting a degree of specificity in neuronal targeting by the chimera. (C) Confocal microscopy images of cultured dorsal root ganglion neurons, exposed to both the clostridial chimera and IB4 lectin, demonstrate that the clostridial chimera targets an IB4-lectin negative subpopulation of the sensory cells.

mammals and yet efficiently blocks CNS functions. The rational design of the chimera depended on three basic pieces of knowledge. First, the botulinum enzyme together with its translocation domain is highly effective in causing long-lasting blockade of neurotransmitter release.<sup>1</sup> Second, introduction of the linking system within the redesigned botulinum molecule significantly diminishes its paralytic activity.<sup>13</sup> Third, the tetanus binding domain targets central neurons without affecting the neurotransmitter release machinery at neuromuscular junctions.<sup>10</sup> Combination of these three properties allowed us to achieve a nonparalytic neuronal blocking agent.

The potential uses of the new clostridial chimera for neurobiology and medicine are likely to be diverse: here we would like to highlight several potential applications. First, native botulinum toxin type A (e.g., BOTOX, Allergan) is now used for the treatment of chronic migraine. Although BOTOX efficiently induces neuromuscular paralysis in all patients injected, only half report adequate relief from migraine symptoms.<sup>33,34</sup> This result suggests that the medicinal properties of botulinum molecules

are not always based on their paralytic action at neuromuscular junctions. Indeed, we and others have reported that peripheral injections of clostridial molecules can affect a diverse set of neurons, ranging from sensory primary afferents to central neurons.<sup>3,35,36</sup> Clearly, a nonparalytic molecule which targets specific neurons will be invaluable in delineating the neuronal circuits that are important in chronic pain conditions. Further work on a wide variety of pain conditions (neuropathic, inflammatory, postoperative symptoms, etc.) will be necessary to provide new insights into the mechanisms of pain generation, its longevity, and potential treatment. Second, a sizable proportion of people with epilepsy suffer from drug-resistant focally generated seizures, with surgical removal of the affected brain areas being the only option to treat some of these patients.<sup>37,38</sup> It can be envisioned that safe delivery of a nonparalytic clostridial chimera into spatially defined regions measuring as little as one cubic millimeter might be effective in blocking seizure-generating areas for several months. Such a silencing effect could be a relatively noninvasive means of predicting the likelihood that surgery would be successful, and might even be sufficiently effective to rewire and permanently disable seizure-generating circuits, thereby avoiding the need for surgery.

Here, we have demonstrated for the first time that the newly introduced ‘protein stapling’ technique allows creation of a safe neuronal blocking agent. Development of new synthetic neuronal blocking agents with enhanced functions which can be injected into desired areas opens new avenues for probing nerve functions not only in rodents, but also in higher organisms—a requirement in our quest to understand the human brain.<sup>39,40</sup>

## AUTHOR INFORMATION

### Corresponding Author

\*E-Mail: b.davletov@sheffield.ac.uk; Tel.: +44-114-2225111.

### Author Contributions

Enrico Ferrari, Chunjing Gu, Dhevahii Niranjan contributed equally to the study.

### Notes

The authors declare no competing financial interest.

## ACKNOWLEDGMENTS

This study was supported by the MRC grant U10578791 and Wellcome Trust Grant No. 089125/Z/09/Z. We thank David Menon and Peter McNaughton for helpful discussions. We thank Richard Berks, Claire Knox, and Angela Middleton for their help with the biological tests.

## ABBREVIATIONS

AFM, Atomic Force Microscopy; ANOVA, Analysis of Variance; BoNT/A, Botulinum Neurotoxin type A; CFA, Complete Freund’s Adjuvant; CNS, Central Nervous System; DRG, Dorsal Root Ganglia; HBSS, Hanks’s Balanced Salt Solution; HRP, Horseradish Peroxidase; MEM, Minimum Essential Medium; NGF, Nerve growth factor; PBS, Phosphate Buffered Saline; SDS, Sodium Dodecyl Sulfate; SDS-PAGE, Sodium Dodecyl Sulfate; PAGE, Polyacrylamide Gel Electrophoresis; SEM, Standard Error of the Mean; SNAP-25, Synaptosomal-associated protein of 25 kDa; SNARE, SNAP Soluble NSF Attachment Protein Receptor; TAMRA, Carboxytetramethylrhodamine; TBD, Tetanus Binding Domain; VEP, Visual Evoked Potential

## REFERENCES

- (1) Foster, K. A. (2009) Engineered Toxins: New Therapeutics. *Toxicon* 54, 587–592.
- (2) Dolly, J. O., Lawrence, G. W., Meng, J., Wang, J., and Ovsepian, S. V. (2009) Neuro-Exocytosis: Botulinum Toxins as Inhibitory Probes and Versatile Therapeutics. *Curr. Opin. Pharmacol.* 9, 326–335.
- (3) Stockel, K., Schwab, M., and Thoenen, H. (1975) Comparison Between the Retrograde Axonal Transport of Nerve Growth Factor and Tetanus Toxin in Motor, Sensory and Adrenergic Neurons. *Brain Res* 99, 1–16.
- (4) Davletov, B., Bajohrs, M., and Binz, T. (2005) Beyond BOTOX: Advantages and Limitations of Individual Botulinum Neurotoxins. *Trends Neurosci.* 28, 446–452.
- (5) Binz, T., and Rummel, A. (2009) Cell Entry Strategy of Clostridial Neurotoxins. *J. Neurochem.* 109, 1584–1595.
- (6) Südhof, T. C., and Rothman, J. E. (2009) Membrane Fusion: Grappling with SNARE and SM Proteins. *Science* 323, 474–477.
- (7) Meunier, F. A., Schiavo, G., and Molgó, J. (2002) Botulinum Neurotoxins: From Paralysis to Recovery of Functional Neuromuscular Transmission. *J. Physiol. (Paris)* 96, 105–113.
- (8) Fernández-Chacón, R., and Südhof, T. C. (1999) Genetics of Synaptic Vesicle Function: Toward the Complete Functional Anatomy of an Organelle. *Annu. Rev. Physiol.* 61, 753–776.
- (9) Chao, M. V. (2003) Retrograde Transport Redux. *Neuron* 39, 1–2.
- (10) Schiavo, G., Matteoli, M., and Montecucco, C. (2000) Neurotoxins Affecting Neuroexocytosis. *Physiol. Rev.* 80, 717–766.
- (11) McMahon, H. T., Foran, P., Dolly, J. O., Verhage, M., Wiegant, V. M., and Nicholls, D. G. (1992) Tetanus Toxin and Botulinum Toxins Type A and B Inhibit Glutamate, Gamma-Aminobutyric Acid, Aspartate, and Met-Enkephalin Release from Synaptosomes. Clues to the Locus of Action. *J. Biol. Chem.* 267, 21338–21343.
- (12) Darios, F., Niranjan, D., Ferrari, E., Zhang, F., Soloviev, M., Rummel, A., Bigalke, H., Suckling, J., Ushkaryov, Y., Naumenko, N., Shakiryanova, A., Giniatullin, R., Maywood, E., Hastings, M., Binz, T., and Davletov, B. (2010) SNARE Tagging Allows Stepwise Assembly of a Multimodular Medicinal Toxin. *Proc. Natl. Acad. Sci. U.S.A.* 107, 18197–18201.
- (13) Ferrari, E., Maywood, E. S., Restani, L., Caleo, M., Pirazzini, M., Rossetto, O., Hastings, M. H., Niranjan, D., Schiavo, G., and Davletov, B. (2011) Re-Assembled Botulinum Neurotoxin Inhibits CNS Functions without Systemic Toxicity. *Toxins* 3, 345–355.
- (14) Kaech, S., and Bunker, G. (2006) Culturing Hippocampal Neurons. *Nat. Protoc.* 1, 2406–2415.
- (15) Harper, C. B., Martin, S., Nguyen, T. H., Daniels, S. J., Lavidis, N. A., Popoff, M. R., Hadzic, G., Mariana, A., Chau, N., McCluskey, A., Robinson, P. J., and Meunier, F. A. (2011) Dynamin Inhibition Blocks Botulinum Neurotoxin Type A Endocytosis in Neurons and Delays Botulism. *J. Biol. Chem.* 286, 35966–35976.
- (16) Yoo, S. H., Yamazaki, S., Lowrey, P. L., Shimomura, K., Ko, C. H., Buhr, E. D., Siepka, S. M., Hong, H. K., Oh, W. J., Yoo, O. J., Menaker, M., and Takahashi, J. S. (2004) PERIOD2::LUCIFERASE Real-Time Reporting of Circadian Dynamics Reveals Persistent Circadian Oscillations in Mouse Peripheral Tissues. *Proc. Natl. Acad. Sci. U.S.A.* 101, 5339–5346.
- (17) Maywood, E. S., Reddy, A. B., Wong, G. K., O’Neill, J. S., O’Brien, J. A., McMahon, D. G., Harmar, A. J., Okamura, H., and Hastings, M. H. (2006) Synchronization and Maintenance of Timekeeping in Suprachiasmatic Circadian Clock Cells by Neuropeptidergic Signaling. *Curr. Biol.* 16, 599–605.
- (18) Rasetti-Escargueil, C., Jones, R. G., Liu, Y., and Sesardic, D. (2009) Measurement of Botulinum Types A, B and E Neurotoxicity Using the Phrenic Nerve-Hemidiaphragm: Improved Precision with In-Bred Mice. *Toxicon* 53, 503–511.
- (19) Cerri, C., Fabbri, A., Vannini, E., Spolidoro, M., Costa, M., Maffei, L., Fiorentini, C., and Caleo, M. (2011) Activation of Rho GTPases Triggers Structural Remodeling and Functional Plasticity in the Adult Rat Visual Cortex. *J. Neurosci.* 31, 15163–15172.
- (20) Restani, L., Cerri, C., Pietrasanta, M., Gianfranceschi, L., Maffei, L., and Caleo, M. (2009) Functional Masking of Deprived Eye

- Responses by Callosal Input during Ocular Dominance Plasticity. *Neuron* 64, 707–718.
- (21) Caleo, M., Medini, P., von Bartheld, C. S., and Maffei, L. (2003) Provision of Brain-Derived Neurotrophic Factor via Anterograde Transport from the Eye Preserves the Physiological Responses of Axotomized Geniculate Neurons. *J. Neurosci.* 23, 287–296.
- (22) Caleo, M., Restani, L., Gianfranceschi, L., Costantin, L., Rossi, C., Rossetto, O., Montecucco, C., and Maffei, L. (2007) Transient Synaptic Silencing of Developing Striate Cortex Has Persistent Effects on Visual Function and Plasticity. *J. Neurosci.* 27, 4530–4540.
- (23) Restani, L., Antonucci, F., Gianfranceschi, L., Rossi, C., Rossetto, O., and Caleo, M. (2011) Evidence for Anterograde Transport and Transcytosis of Botulinum Neurotoxin A (BoNT/A). *J. Neurosci.* 31, 15650–15659.
- (24) Ferrari, E., Soloviev, M., Niranjan, D., Arsenault, J., Gu, C., Vallis, Y., O'Brien, J., and Davletov, B. (2012) Assembly of Protein Building Blocks Using a Short Synthetic Peptide. *Bioconjugate Chem.* 23, 479–484.
- (25) Rossi, E. A., Goldenberg, D. M., and Chang, C. (2012) The Dock-and-Lock Method Combines Recombinant Engineering with Site-Specific Covalent Conjugation To Generate Multifunctional Structures. *Bioconjugate Chem.* 23, 309–323.
- (26) Yeh, F. L., Dong, M., Yao, J., Tepp, W. H., Lin, G., Johnson, E. A., and Chapman, E. R. (2010) SV2Mediates Entry of Tetanus Neurotoxin into Central Neurons. *PLoS Pathog.* 6, e1001207.
- (27) Matteoli, M., Verderio, C., Rossetto, O., Iezzi, N., Coco, S., Schiavo, G., and Montecucco, C. (1996) Synaptic Vesicle Endocytosis Mediates the Entry of Tetanus Neurotoxin into Hippocampal Neurons. *Proc. Natl. Acad. Sci. U.S.A.* 93, 13310–13315.
- (28) Jones, R. G., Ochiai, M., Liu, Y., Ekong, T., and Sesardic, D. (2008) Development of Improved SNAP25 Endopeptidase Immuno-Assays for Botulinum Type A and E Toxins. *J. Immunol. Methods* 329, 1384–1391.
- (29) Mandolesi, G., Menna, E., Harauzov, A., von Bartheld, C. S., Caleo, M., and Maffei, L. (2005) A Role for Retinal Brain-Derived Neurotrophic Factor in Ocular Dominance Plasticity. *Curr. Biol.* 15, 2119–2124.
- (30) Dolly, J. O., Wang, J., Zurawski, T. H., and Meng, J. (2011) Novel Therapeutics Based on Recombinant Botulinum Neurotoxins to Normalize the Release of Transmitters and Pain Mediators. *FEBS J.* 278, 4454–4466.
- (31) Arunachalam, L., Han, L., Tassew, N. G., He, Y., Wang, L., Xie, L., Fujita, Y., Kwan, E., Davletov, B., Monnier, P. P., Gaisano, H. Y., and Sugita, S. (2008) Munc18–1 Is Critical for Plasma Membrane Localization of Syntaxin1 but not of SNAP-25 in PC12 Cells. *Mol. Biol. Cell* 19, 722–734.
- (32) Cavanaugh, D. J., Lee, H., Lo, L., Shields, S. D., Zylka, M. J., Basbaum, A. I., and Anderson, D. J. (2009) Distinct Subsets of Unmyelinated Primary Sensory Fibers Mediate Behavioral Responses to Noxious Thermal and Mechanical Stimuli. *Proc. Natl. Acad. Sci. U.S.A.* 106, 9075–9080.
- (33) Petri, S., Tölle, T., Straube, A., Pfaffenrath, V., Stefenelli, U., and Ceballos-Baumann, A. (2009) Botulinum Toxin as Preventive Treatment for Migraine: a Randomized Double-Blind Study. *Eur. Neurol.* 62, 204–211.
- (34) Silberstein, S., Mathew, N., Saper, J., and Jenkins, S. (2000) Botulinum Toxin Type A as a Migraine Preventive Treatment. *Headache* 40, 445–450.
- (35) Caleo, M., and Schiavo, G. (2009) Central Effects of Tetanus and Botulinum Neurotoxins. *Toxicon* 54, 593–599.
- (36) Bilsland, L. G., Sahai, E., Kelly, G., Golding, M., Greensmith, L., and Schiavo, G. (2010) Deficits in Axonal Transport Precede ALS Symptoms in Vivo. *Proc. Natl. Acad. Sci. U.S.A.* 107, 20523–20528.
- (37) Berg, A. T., Matherne, G. W., Bronen, R. A., Fulbright, R. K., Di Mario, F., Testa, F. M., and Levy, S. R. (2009) Frequency, Prognosis and Surgical Treatment of Structural Abnormalities Seen with Magnetic Resonance Imaging in Childhood Epilepsy. *Brain* 132, 2785–2797.
- (38) Engel, J., Jr., McDermott, M. P., Wiebe, S., Langfitt, J. T., Stern, J. M., Dewar, S., Sperling, M. R., Gardiner, I., Erba, G., Fried, I., Jacobs, M., Vinters, H. V., Mintzer, S., and Kieburtz, K. (2012) Early Surgical Therapy for Drug-Resistant Temporal Lobe Epilepsy: a Randomized Trial. *JAMA* 307, 922–930.
- (39) Woodruff, A., and Yuste, R. (2008) Of Mice and Men, and Chandeliers. *PLoS Biol.* 6, e243.
- (40) Ellis-Behnke, R. G., Teather, L. A., Schneider, G. E., and So, K. F. (2007) Using Nanotechnology to Design Potential Therapies for CNS Regeneration. *Curr. Pharm. Des.* 13, 2519–2528.